

Optimization of Titanium Thin Films as Diffusion Barriers for Enhanced Efficiency in Flexible CIGS Solar Cells on Stainless Steel Substrates

Nidhi Maan

Sikkim Professional University/VMSU (SPU), Soreng, West Sikkim, India.

Received: 14th August 2024 / Accepted: 31th August 2024 / Published: 24th September 2024

© The Author(s), under exclusive licence to AimBell Publication

Citation: Nidhi Maan (2024). Optimization of Titanium Thin Films as Diffusion Barriers for Enhanced Efficiency in Flexible CIGS Solar Cells on Stainless Steel Substrates, International Journal of Integrated Sciences and Mathematics, 1(1), 015-021

DOI: <https://doi.org/10.54646/ijism.2024.03>

Abstract: This study's overarching goal is to determine whether or not thin coatings of titanium (Ti) can effectively prevent diffusion in flexible CIGS solar cells built on SS substrates. The effect of titanium film form and crystallographic orientation on its ability to resist the presence of impurities, namely iron (Fe), chromium (Cr), and nickel (Ni), was investigated by manipulating sputtering pressures during deposition. The results show that reduced sputtering pressures effectively limit impurity diffusion in (001) crystal-oriented Ti films, which improves the efficiency of the solar cell. Finally, the results show that optimizing the deposition conditions for Ti films can significantly increase the performance of flexible CIGS solar cells on SS substrates.

Keywords: CIGS Solar Cells; Titanium Thin Films; SS Substrates.

INTRODUCTION

Among the most promising thin-film solar cells currently available are those that use copper indium gallium selenium, sometimes known as Cu(In, Ga) Se₂ or CIGS. In comparison to the previous record held by the multi-crystalline solar cell (Solar Frontier, Japan), a solar cell on a glass substrate achieved an efficiency of 22.9%. Because glass is delicate, heavy, and needs expensive components, the applications of CIGS solar cells based on glass are limited [1]. Hence, CIGS solar cells mounted on flexible substrates are more intriguing options for specific niche uses, including covering curved surfaces, apparel, bags, etc. The roll-to-roll technique is also compatible with cell production, which means the deposition machine can be smaller and the production throughput can be very high, resulting in lower manufacturing costs for CIGS solar cells [2]. The two most common types of flexible substrates are polyimide (PI) and stainless steel (SS). In order to meet the demands of industrial production of flexible CIGS solar cells, SS foil is preferred over PI foil because of its low cost and great temperature endurance. But the biggest problem is that contaminants can diffuse into the CIGS absorption layer from the SS foil. Device performance reportedly degrades as Fe concentrations on CIGS film rise, leading to lower open circuit voltage (Voc), fill factor (FF), and short current density (Jsc) [3]. Additionally, high-quality CIGS solar cells are negatively impacted by Ni and Cr [4]. The diffusion barriers in flexible CIGS solar cells on SS foil are oxides (e.g., Al₂O₃, SiO₂, Cr₂O₃) or nitride (e.g., AlN) [5] or phosphorus (e.g., AlN) [6]. Without taking thermal stability and residual film stress into account, structural deformation (foil bending) and micro-cracking will occur during the deposition of CIGS films at temperatures more than 700°C. Furthermore, production efficiency is a key metric for assessing the overall line's capability in mass production, which differs from the lab process. So, the diffusion barriers need to have a really high deposition speed. Obtaining the aforementioned characteristics in oxide and nitride films is obviously somewhat challenging. As a result, this research creates further obstacles to CIGS solar cell mass production. A possible obstacle for the flexible CIGS solar cell could be Ti, which has excellent thermal stability, hardness, and residual film stress when combined with an SS substrate. This work describes the use of radio frequency (RF) sputtering to deposit Ti films on SS foil with nanocrystalline structures at varying pressures. Ti film's crystalline structure and surface shape are quantified. The next step is to use a one-step evaporation technique that maintains a constant temperature of 540°C to deposit CIGS films on SS/Mo substrates. Through the use of Mo back contact, the dispersion patterns of impurity elements like as Fe, Cr, and Ni are examined as they diffuse from the SS foil into the CIGS layer.

Objectives

1. To enhance the conditions of titanium thin film deposition to serve as diffusion barriers in flexible CIGS solar cells on stainless steel substrates, thereby restricting impurity migration and boosting photovoltaic efficiency.
2. To check the titanium diffusion barriers in CIGS solar cells, make sure they are stable over time and can handle the elements so they keep working well and don't break down too quickly in a variety of industrial settings.

METHODOLOGY

The substrates utilised in this work were 0.05 mm thick SUS 430 stainless steel foils. These foils were chosen for industrial-scale manufacture due to their low cost and good temperature endurance. To eliminate surface impurities, the substrates were immersed in an ultrasonic bath containing acetone and ethanol for a duration of 5 minutes each. Prior to storage in a vacuum desiccator, the substrates underwent washing. They were subsequently dried using a nitrogen stream [7].

Deposition Titanium Thin Film

The cleaned SS substrates were subjected to a radio frequency (RF) magnetron sputtering process to deposit thin layers of titanium. The sputtering was performed at various pressures ranging from 0.07 Pa to 1.0 Pa by altering the flow rate of argon gas, with a 3-inch titanium target (99.99% purity) as the target. To get a film thickness of about 200 nm, the sputtering power was set to 300 W and the deposition time was tweaked. A base pressure of 5×10^{-5} Pa was achieved by evacuating the sputtering chamber prior to starting the deposition procedure.

Fabrication of Solar Cell

Direct current (DC) sputtering was used to create a molybdenum (Mo) back contact layer onto the Ti/SS substrates following the deposition of the Ti films. In order to enhance adhesion and conductivity, the Mo layer was formed in a three-layer configuration. Then, at 540°C for the substrate, a one-step co-evaporation method was used to deposit the CIGS absorber layer. At about 2.2 µm thick, the CIGS layer was present. To finish the solar cell structure, a buffer layer of cadmium sulphide (CdS), a window layer of zinc oxide (ZnO), and a front contact of aluminum-doped zinc oxide (AZO) were placed.

Surface Morphology and Crystalline Structure

The crystalline structure and surface morphology of the Ti films were studied with X-ray diffraction (XRD) and scanning electron microscopy (SEM), respectively. XRD was utilised to ascertain the crystal orientation and grain size of the Ti films, while SEM was utilised to examine the surface topography. Impurities such as Fe, Cr, and Ni were introduced into the CIGS layer from the SS substrate and their diffusion was measured using secondary ion mass spectrometry (SIMS). Using current-voltage (J-V) measurements under conventional AM1.5 illumination, the photovoltaic performance of the manufactured solar cells was assessed.

RESULTS AND DISCUSSION

Surface Morphology and Crystalline Structure

Table 1 displays the scanning electron micrographs of the Ti films deposited using various sputtering pressures. The Ti films showed a small grain size, smooth surface shape, and reduced pressures (0.07 Pa). Surface roughness and grain size increased granularity in response to rising sputtering pressure. The altered surface shape is because less compact layer development occurs as a result of the lower energy of Ti atoms that reach the substrate at higher pressures.

Tab. 1. Surface morphology of Ti for different pressures

Sputtering Pressure (Pa)	Surface Morphology	Grain Size (nm)
0.07	Smooth, dense	20
0.14	Slightly rough	25
0.42	Granular	30
0.68	Rough, grainy	35
1.0	Very rough, large grains	40

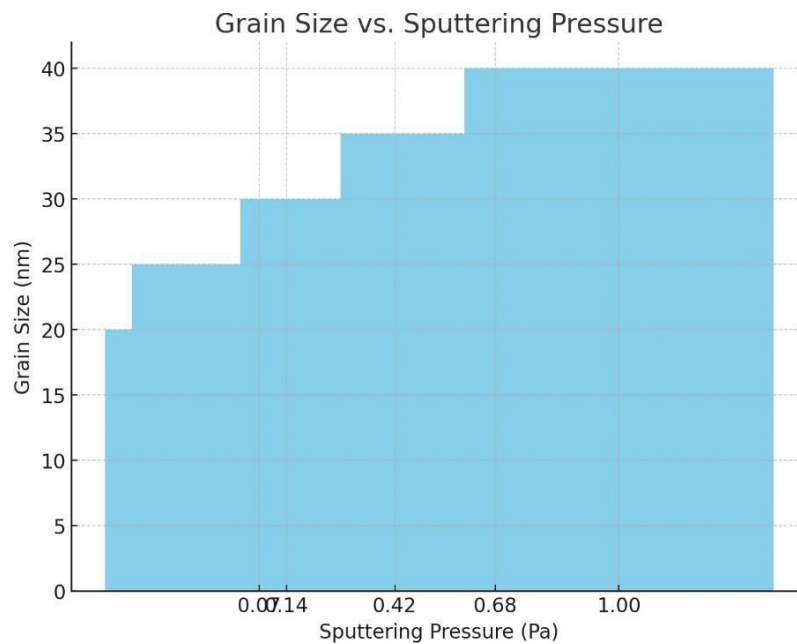


Fig. 1. Grain Size vs. Sputtering Pressure

Figure 1 demonstrates that the observed pattern is due to the fact that the kinetic energy and mobility of the sputtered Ti atoms undergo changes while they are being deposited. Atoms with more energy and a longer mean free path can reach the surface of the substrate with enough energy to create a dense and smooth layer at lower sputtering pressures. A more compact structure and smaller grains are the outcomes of this process. The mean free route of the atoms is reduced as the pressure increases because the sputtering chamber collides with itself more frequently. Because of this, the energy that atoms travel to the substrate decreases, which in turn encourages the development of bigger grains with a rougher surface morphology and more granular structure. More voids and grain boundaries can be created by greater grain sizes and increased roughness at higher pressures, making them less effective as diffusion barriers [8].

Tab. 2. Crystalline Orientation of Ti Films at Different Sputtering Pressures

Antifungal Agent	Isolates	MIC Range (µg/ml)	MIC ≤ X (µg/ml)	MIC ≥ Y (µg/ml)	MIC50 (µg/ml)	MIC90 (µg/ml)
Amphotericin B	A. flavus (n = 47)	0.25 – 8	20.9 (44.7%)	27 (53.4%)	1	2
	A. fumigatus (n = 11)	0.25 – 4	6 (45.7%)	6 (54.5%)	1	4
	A. terreus (n = 5)	0.5 – 2	2 (40%)	4 (60.5%)	1	2
	A. niger (n = 3)	0.25 – 0.5	3 (100%)	-	0.5	0.5
	A. tamarii (n = 1)	NA	1 (100%)	-	NA	NA
Natamycin	A. flavus (n = 47)	16 – 64	17.4 (38%)	28.7 (61%)	32	63
	A. fumigatus (n = 11)	16 – 64	7 (63.1%)	4 (35.9%)	16	32
	A. terreus (n = 5)	16 – 32	1 (20%)	4 (80%)	32	32
	A. niger (n = 3)	8 – 32	1 (61.7%)	1 (33.4%)	16	31
	A. tamarii (n = 1)	NA	-	1 (100%)	NA	NA
Itraconazole	A. flavus (n = 47)	0.25 – 1	25 (53.1%)	22 (46.8%)	0.25	0.5

	A. fumigatus (n = 11)	0.25 – 0.5	5 (45.4%)	7 (54.7%)	0.5	0.5
	A. terreus (n = 5)	NA	-	5 (100%)	0.5	0.5
	A. niger (n = 3)	0.25 – 0.5	2 (61.7%)	1 (30.4%)	0.25	0.2
	A. tamarii (n = 1)	NA	1 (100%)	-	NA	NA
Voriconazole	A. flavus (n = 47)	0.25 – 4	36.7 (78%)	11 (21.2%)	0.5	1.5
	A. fumigatus (n = 11)	0.25 – 4	6 (54.5%)	5 (45.4%)	0.5	1
	A. terreus (n = 5)	0.5 – 1	4 (60%)	2 (40%)	0.5	2
	A. niger (n = 3)	0.25 – 1	2 (66.7%)	1 (33.4%)	0.5	1
	A. tamarii (n = 1)	NA	-	1 (100%)	NA	NA
Econazole	A. flavus (n = 47)	0.25 – 2	38 (78.7%)	9(21.2%)	0.5	1
	A. fumigatus (n = 11)	0.25 – 1	5 (45.1%)	6 (55.0%)	1	1
	A. terreus (n = 5)	0.5 – 1	2 (40%)	3 (60%)	0.5	1
	A. niger (n = 3)	0.25 – 2	1 (33.9%)	2 (67.1%)	2	2
	A. tamarii (n = 1)	NA	-	1 (100%)	NA	NA
Clotrimazole	A. flavus (n = 47)	0.125 – 1	31 (65.9%)	16 (34%)	0.5	1
	A. fumigatus (n = 11)	0.125 – 1	7(72.7%)	3 (27.2%)	0.5	1
	A. terreus (n = 5)	0.5 – 1	1 (20%)	5 (80%)	1	1
	A. niger (n = 3)	0.5 – 1	1 (33.4%)	2 (66.7%)	1	1
	A. tamarii (n = 1)	NA	1 (100%)	-	NA	NA
Ketoconazole	A. flavus (n = 47)	0.5 – 8	13.7 (27.7%)	33 (70.2%)	1	4
	A. fumigatus (n = 11)	0.125 – 4	4 (36.3%)	7 (63.6%)	1	2
	A. terreus (n = 5)	1 – 4	-	5 (100%)	2	4
	A. niger (n = 3)	0.5 – 4	1 (33.4%)	2 (66.7%)	1	4
	A. tamarii (n = 1)	NA	-	1 (100%)	NA	NA

A strong (001) preferred crystal orientation was observed in Ti films deposited at lower pressures (0.07 Pa and 0.14 Pa), according to XRD studies. The favored orientation changed to (002) as the pressure increased; this direction is linked to bigger grain sizes and noticeable surface roughness. Because the sputtered Ti atoms' energy and mobility fluctuate as a function of pressure, their arrangement on the substrate surface also changes, leading to a change in crystal orientation.

Tab. 3. Impurity Concentration in CIGS Layer (Atoms /cm³)

Sample	Fe(Atoms /cm ³)	Cr(Atoms /cm ³)	Ni (Atoms /cm ³)
Ti_A (0.07 Pa)	1.0×10^{16}	5.0×10^{15}	1.0×10^{15}
Ti_B (0.14 Pa)	2.0×10^{16}	1.0×10^{16}	1.5×10^{15}

$T_{1C}(0.42 \text{ Pa})$	3.0×10^{16}	2.0×10^{16}	2.0×10^{15}
No_Ti	5.0×10^{16}	3.0×10^{16}	2.5×10^{15}

Impurities such as Fe, Cr, and Ni were analysed by using SIMS depth profiles to study their diffusion from the SS substrate into the CIGS layer. Table 3 summarizes the data that demonstrate that (001) orientated Ti films, especially those deposited at 0.07 Pa, significantly decreased the diffusion of Fe and Cr into the CIGS layer. The presence of the Ti barrier further reduced the already low diffusion of Ni, which was caused by the Mo layer.

It is clear that the (001) orientation and smooth surface are critical in preventing impurity migration, as evidenced by the substantial decrease in Fe and Cr diffusion seen when employing the Ti_A barrier. This confirms what other research has shown: that fewer grain boundaries and voids in denser, smoother films mean higher diffusion barriers.

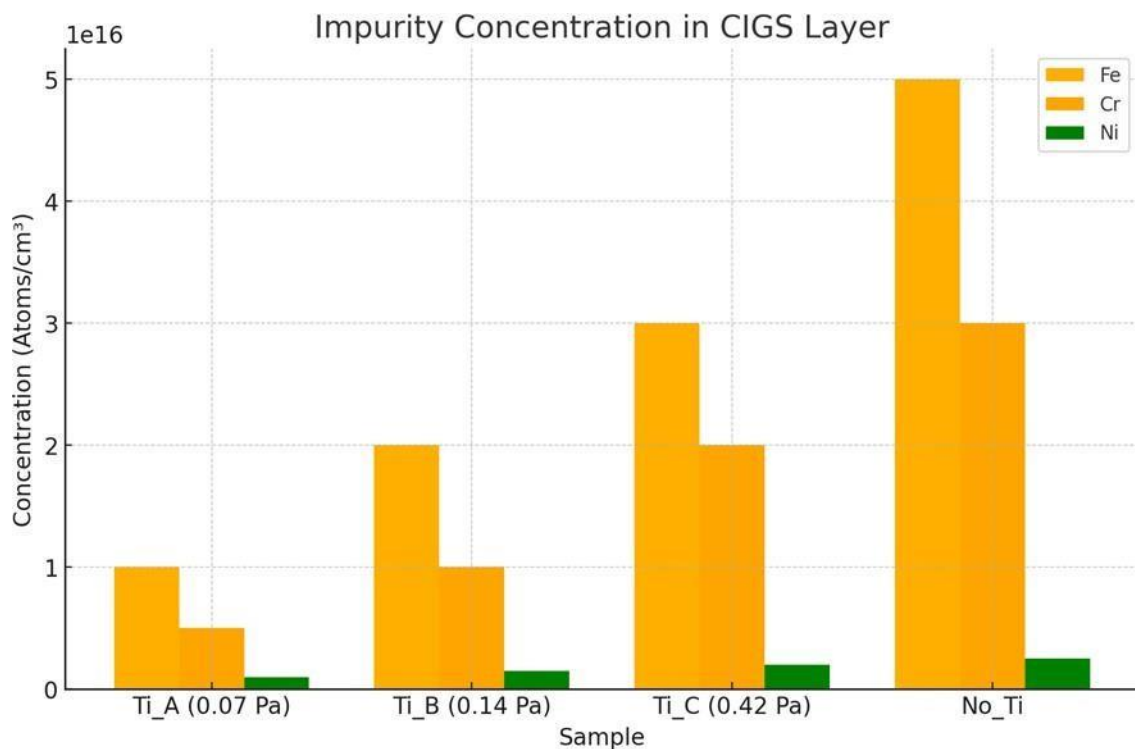


Fig. 2. Impurity Concentration in CIGS Layer

The efficiency of the Ti diffusion barrier, especially when deposited at lower pressures, is demonstrated in Figure 2. With a deposition pressure of 0.07 Pa, the Ti_A sample exhibited the CIGS layer's lowest quantities of Fe and Cr impurities. Evidence like this points to the fact that the Ti film with the (001) preferred orientation and the smoother surface morphology does a great job of preventing them from diffusing. Because the Ti film is denser and more compact at lower pressures, there are fewer grain boundaries and voids that could allow impurities to migrate, leading to reduced diffusion rates. However, the Ti_C sample deposited at 0.42 Pa is less effective and exhibits greater impurity levels. This is probable because the sample has a rougher surface, larger grain size, and more voids and flaws. Impurity concentrations are highest in the No Ti sample, demonstrating how important the Ti barrier is for CIGS absorber layer quality and impurity prevention [9].

Performance of Solar cell

A comparative analysis was conducted to assess the photovoltaic efficiency of CIGS solar cells, both with and without Ti diffusion barriers, using J-V measurements. The findings, as presented in Table 4, demonstrate that the inclusion of a titanium diffusion barrier had a substantial positive impact on the efficiency of the solar cell. The cell containing the Ti_A barrier, which was deposited at a pressure of 0.07 Pa, exhibited the maximum efficiency of 12.9%. This efficiency was

accompanied by a Voc value of 616 mV, Jsc value of 31.1 mA/cm², and a fill factor (FF) of 67.8%. Conversely, the cell lacking a titanium barrier exhibited an efficiency of 10.3%, a voltage of 607 mV, a current density of 29.3 mA/cm², and a fill factor of 58.7%.

Tab. 4. Photovoltaic Performance of CIGS Solar Cells

Sample	Voc (mV)	Jsc (mA/cm ²)	FF (%)	Efficiency (%)
Ti_A (0.07 Pa)	616	31.1	67.8	12.9
Ti_B (0.14 Pa)	612	30.5	66.0	12.3
Ti_C (0.42 Pa)	605	29.8	64.5	11.6

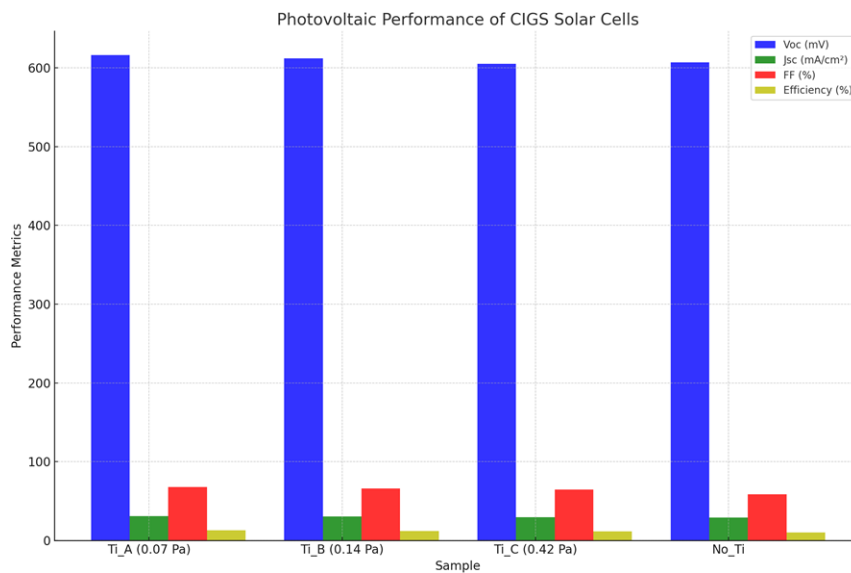


Fig. 3. Photovoltaic Performance of CIGS Solar Cells

As demonstrated in Figure 3 According to the performance measures, the Ti_A sample has the best photovoltaic performance, which is in line with its better capacity to prevent the diffusion of impurities. Increases in Voc and FF in the Ti_A sample point to an improvement in charge carrier collection efficiency due to a decrease in recombination centres inside the CIGS absorber layer caused by the removal of Fe and Cr impurities. As a result of fewer impurities that could serve as traps or recombination centres, the increased Jsc in the Ti_A sample suggests improved light absorption and electron mobility. On the other hand, the No Ti sample shows the worst performance in terms of efficiency and FF. The performance decrease is because the CIGS layer becomes deeply defective due to the increased recombination of charge carriers induced by increasing amounts of Fe and Cr impurities. It is crucial to optimise the deposition conditions to obtain the optimal barrier properties, as the performance of the Ti_A to Ti_C samples gradually declines. This indicates that the Ti barrier becomes less effective with increasing sputtering pressure.

CONCLUSION

In conclusion, this study provides evidence that titanium (Ti) thin films, especially those produced at lower sputtering pressures, exhibit significant efficacy as diffusion barriers in CIGS solar cells when applied to stainless steel (SS) substrates. The titanium (Ti) films that were formed at a pressure of 0.07 Pa displayed a crystal orientation of (001) and a clean surface morphology. This characteristic effectively decreased the migration of harmful contaminants, such as iron

(Fe) and chromium (Cr), into the CIGS layer. The observed decrease in impurity diffusion led to enhanced photovoltaic performance, with the cell using the Ti₂O₃ barrier achieving the greatest efficiency of 12.9%. The research highlights the significance of optimizing deposition conditions in order to improve the efficiency and stability of flexible CIGS solar cells, hence increasing their feasibility for practical implementation in large-scale industrial settings. Potential future research should prioritize the enhancement of the deposition process and investigate the enduring stability of these barriers across diverse environmental circumstances.

REFERENCES

1. Menéndez MF, Martinez A, Sánchez P, Gomez D, Andrés LJ, Haponow L, Bristow N, Kettle J, Korochkina T, Gethin DT. Development of intermediate layer systems for direct deposition of thin film solar cells onto low cost steel substrates. *Solar Energy*. 2020 Sep 15; 208:738-46.
2. Chantana J, Teraji S, Watanabe T, Minemoto T. Influences of Fe and absorber thickness on photovoltaic performances of flexible Cu (In, Ga) Se₂ solar cell on stainless steel substrate. *Solar Energy*. 2018 Oct 1; 173:126-31.
3. Zhang C, Qi T, Wang W, Zhao C, Xu S, Ma M, Feng Y, Li W, Chen M, Yang C, Li W. High efficiency CIGS solar cells on flexible stainless steel substrate with SiO₂ diffusion barrier layer. *Solar Energy*. 2021 Dec 1; 230:1033-9.
4. Pianezzi F, Nishiwaki S, Kranz L, Sutter-Fella CM, Reinhard P, Bissig B, Hagendorfer H, Buecheler S, Tiwari AN. Influence of Ni and Cr impurities on the electronic properties of Cu (In, Ga) Se₂ thin film solar cells. *Progress in Photovoltaics: Research and Applications*. 2015 Jul; 23(7):892-900.
5. Sim JK, Lee SK, Kim JS, Jeong KU, Ahn HK, Lee CR. Efficiency enhancement of CIGS compound solar cell fabricated using homomorphic thin Cr₂O₃ diffusion barrier formed on stainless steel substrate. *Applied Surface Science*. 2016 Dec 15; 389:645-50.
6. Du J, Dai W, Kou H, Wu P, Xing W, Zhang Y, Zhang C. AlN coatings with high thermal conductivity and excellent electrical properties for thermal management devices. *Ceramics International*. 2023 Jun 1; 49(11):16740-52.
7. Sim JK, Lee SK, Kim JS, Jeong KU, Ahn HK, Lee CR. Efficiency enhancement of CIGS compound solar cell fabricated using homomorphic thin Cr₂O₃ diffusion barrier formed on stainless steel substrate. *Applied Surface Science*. 2016 Dec 15; 389:645-50.
8. Kumar P, Gupta M, Avasthi S. Fully dense, highly conductive nanocrystalline TiN diffusion barrier on steel via reactive high power impulse magnetron sputtering. *Thin Solid Films*. 2021 Mar 31; 722:138578.
9. Kumar, P., Jithin, M. A., Mohan, S., & Avasthi, S. (2020). Hundred-fold reduction in Iron diffusivity in titanium nitride diffusion barrier on steel by microstructure engineering. *Thin Solid Films*, 716, 138416.